

Comparative aspects of temporal bone pneumatization in some African fossil hominins

Aspects comparatifs de la pneumatisation de l'os temporal chez quelques hominins fossiles africains

A. Balzeau

Received: 13 January 2015; Accepted: 26 March 2015
© Société d'anthropologie de Paris et Lavoisier SAS 2015

Abstract Knowledge on variations in temporal bone pneumatization in fossil hominins is still limited, although this feature could have implications for phylogenetic discussions and more generally for a better understanding of the development of temporal bone anatomy, including specific particularities. Here, we document the pattern of distribution of temporal bone pneumatization in early African hominins attributed to *Australopithecus*, *Paranthropus*, early *Homo* and African *Homo ergaster/Homo erectus*. Contrary to previous suggestions, the specimens analysed here and attributed to *Australopithecus africanus* and *Paranthropus* do not share the ape-like pattern of pneumatization. Further work will contribute to the debate on the developmental and/or functional origin of pneumatization as well as to our understanding of hominin evolution.

Keywords Internal cranial anatomy · Fossil hominins · African great apes · Imaging methodologies

Résumé Les connaissances sur la variation de la pneumatisation de l'os temporal chez les hominins fossiles sont limitées. Pourtant, ce caractère pourrait avoir une utilité pour les discussions phylogénétiques et plus largement pour la compréhension de la mise en place de l'anatomie externe de l'os temporal, et de ses particularités spécifiques. Nous décrivons ici le schéma de distribution de la pneumatisation de l'os temporal chez quelques hominins fossiles africains anciens attribués à différentes espèces des genres *Australopithecus*, *Paranthropus*, « early *Homo* » et à des

Homo ergaster/Homo erectus africains. Contrairement à des suggestions antérieures, les spécimens analysés attribués à *Australopithecus africanus* et *Paranthropus* ne partagent pas le schéma de pneumatisation des grands singes africains. Ces résultats doivent être approfondis et complétés pour contribuer au débat sur l'origine développementale ou fonctionnelle de la pneumatisation mais aussi pour notre compréhension de l'évolution des hominins.

Mots clés Anatomie crânienne interne · Hominins fossiles · Grands singes africains · Méthodes d'imagerie

Introduction

Full descriptions of temporal bone pneumatization patterns are not yet available for all important known fossil hominins. This is particularly true for African specimens. In the case of *Sahelanthropus tchadensis*, *Ardipithecus ramidus*, *Australopithecus afarensis*, *Au. africanus*, *Au. anamensis*, and *Paranthropus aethiopicus*, studies [1-8] have suggested an ape-like pattern of pneumatization, with the appearance of the genus *Homo* characterized by a lower degree of pneumatization [9-10]. According to Nevell and Wood [8], a lower degree of pneumatization of the temporal squama is also observed in *P. robustus*, while the degree of pneumatization in *P. boisei* is variable. This general trend, although derived from diverse sources and restricted material, has been used to support phylogenetic interpretations, as in the case of *Australopithecus sediba* [11]. Temporal bone pneumatization has been widely studied in modern humans, where this feature is highly variable. It is generally limited to the mastoid, perilabyrinthine and petrous regions, and its propagation into the squamous temporal is rare and not extensive [e.g., 12-23]. Recent developments in 3D imaging methodologies were crucial for detailing the pattern of distribution of temporal bone pneumatization in modern humans and in fossil

A. Balzeau (✉)
Equipe de Paléontologie Humaine, UMR 7194 du CNRS,
Département de Préhistoire du Muséum national d'Histoire
naturelle, Musée de l'Homme, Paris, France
e-mail : abalzeau@mnhn.fr

Department of African Zoology,
Royal Museum for Central Africa, Tervuren, Belgium

hominins. Our previous work on Asian *Homo erectus* [24,25] showed that pneumatization is mainly restricted to the area below the supramastoid crest and anterior to the mastoid crest, as well as to the lateral part of the petrous temporal, in the specimens from Ngandong and Sambungmacan. The Zhoukoudian fossils exhibit a unique pattern, with pneumatization distributed across all the areas of the temporal bone. Neandertals [26] share a less asymmetrical pattern of temporal bone pneumatization with modern humans and *Homo erectus* from Ngandong and Sambungmacan, but they have a lower mean volume of pneumatization than modern humans as well as a slightly different pattern of distribution. In particular, pneumatization is slightly less extensive in the anterior and posterior parts of the temporal bone of Neandertals.

Our purpose is to describe the pattern of distribution of temporal bone pneumatization in some early African hominins attributed to *Australopithecus*, *Paranthropus*, early *Homo* and African *Homo ergaster/Homo erectus*. Based on this new evidence, we present a summary of available knowledge concerning temporal bone pneumatization in hominins.

Material and methods

Comparative morphological analyses of the pneumatization of the temporal bone were conducted using computed tomography (CT) data for Sts 5 and 71 (*Au. africanus*), KNM-WT 17000 (*P. aethiopicus*), OH 5 (*P. boisei*), TM 1517 (the type specimen of *Paranthropus robustus*), SK 48 (*P. robustus*), KNM-ER 1805 and 1813 (*H. habilis*), KNM-ER 3733 and 3883, and KNM-WT 15000 (African *H. ergaster/erectus*). The resolution of the data ranges from 0.25 to 1 mm voxel size. This was sufficient to describe the disposition and extent of temporal bone pneumatization but not to compute a 3D quantification. Numerous CT-scans of African great apes were also available, for purposes of comparison, from the collections housed in the Royal Museum for Central Africa [27,28], which contain a total of over 100 specimens. Most of these specimens were collected from the late 19th to the late 20th century in Central Africa, including the Democratic Republic of Congo, Rwanda and Burundi. Many other specimens were collected in Gabon and Cameroon (*Pan troglodytes troglodytes*, *Gorilla gorilla gorilla*) and in Liberia (*Pan troglodytes verus*). The specimens used in this study are all wild individuals. The sex of each specimen is known and all are adults. Information on pneumatization variations in modern humans is from the literature [e.g., 12-23] and from our own publications on the topic [24-26], which also address the morphology of this feature in Neandertals and Asian *H. erectus*.

Based on previous experience, we used CT data to extract information on pneumatization and to describe its extent inside the temporal bone. Pneumatization was reconstructed in three dimensions. The calculation was based on data obtained using a segmentation protocol modified for fossil hominin morphological studies. On each CT slice, the boundary between bone and air (the pneumatic cells) was identified by manual segmentation. This protocol required using multiple threshold values as a function of variation of temporal bone mineralization. The values were also adjusted when sediment was present in the pneumatic cells. These parameters enabled us to obtain precise outlines of the pneumatic cells and thus to produce accurate 3D reconstructions. The various methodological steps were performed using Avizo or Mimics software. The major limitations were the high mineralization and incomplete state of preservation of the internal anatomy of the fossils, and the relatively low resolution of the imaging datasets. Overflow artefacts are present in some specimens and pneumatic cells are occasionally filled with sediment. These problems were partly resolved by using our specific segmentation protocol. We traced the borders of the pneumatized areas only where they could be identified with certainty (Figs 1, 2). We were able to identify the maximal extension of cells in all directions (except medially in the petrous temporal) in nearly all the specimens. Two additional specimens were available (KNM-ER 406, *P. boisei* and OH 9, *H. ergaster/erectus*), but their pneumatization could not be visualized because of the diagenetic alteration of their internal anatomy. Higher-resolution imaging datasets would be necessary in all cases to describe very small features and the extension of the cells more accurately, and more specimens would be welcome. However, the current data, although not perfect, have provided new information on a feature that had not been yet documented in the fossils analyzed.

Results

In Sts 71 (Fig. 1c), the pneumatic cells are concentrated in the mastoid process and in its laterally projecting relief posterior to the external auditory meatus (EAM). Anteriorly, a pneumatic cell is present in the lower part of the temporal squama. It does not connect with the other cells because of the presence of cracks rising vertically above the EAM. There is no indication of pneumatic cell propagation in the rest of the temporal squama. This cell also corresponds to the maximal vertical extension of pneumatization. Pneumatic cells are present along the entire upper border of the EAM. Inferiorly, they have reached the mastoid apex and the upper part of the juxtamastoid eminence. Posteriorly, they have almost reached the occipito-mastoid suture. The disposition and size of the cells indicate that their origin is in the mastoid antrum. It

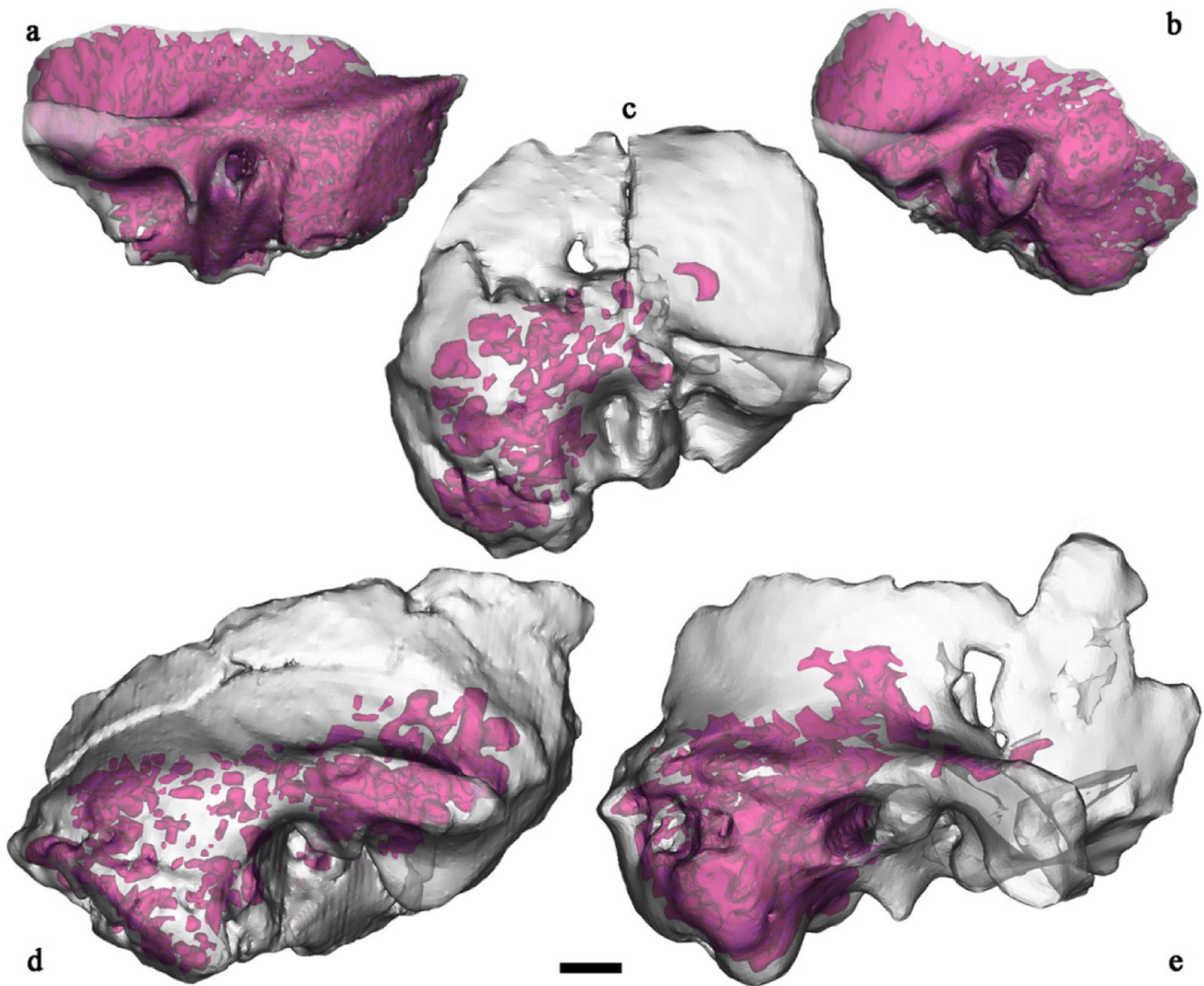


Fig. 1 Lateral views of the 3D reconstructions of the temporal bone and pneumatization: *Gorilla gorilla graueri* (a, female individual, left temporal bone), *Pan paniscus* (b, female individual, type specimen of this species, left temporal bone), Sts 71 (c, right temporal bone), KNM-WT 17000 (d, right temporal bone) and OH 5 (e, right temporal bone). The temporal bones are shown in grey; pneumatization is visible by transparency and is shown in a darker colour. Scale bar = 1 cm / *Vues latérales des reconstructions 3D de l'os temporal et de sa pneumatisation* : *Gorilla gorilla graueri* (a, individu femelle, temporal gauche), *Pan paniscus* (b, individu femelle, spécimen type de l'espèce, temporal gauche), Sts 71 (c, temporal droit), KNM-WT 17000 (d, temporal droit) et OH 5 (e, temporal droit). Les os temporaux sont représentés en gris, la pneumatisation est visible par transparence et représentée en couleur plus foncée. Echelle = 1 cm.

was not possible to reconstruct the pneumatic cells in Sts 5 because of their fragmentary preservation and the presence of sediment with similar mineralization to the fossilized bone. However, their disposition seems to be comparable to that observed in Sts 71. It was not possible to conclude whether the zygomatic process of Sts 71 is pneumatized due to the presence of cracks. In Sts 5, it is evident that the pneumatic cells are confined to the lateral part of the articular tubercle and have not spread into this process.

In KNM-WT 17000 (Fig. 1d), the cells extend anteriorly along the entire inferior extent of the temporal squama in the

area located above the junction with the zygomatic process. They have not spread into the upper part of the temporal squama, or into the medially oriented part of the temporal bone towards the spheno-temporal suture, but have reached into the well-developed zygomatic process. Medially, pneumatization seems to reach the apex of the petrosal. Inferiorly, some pneumatic cells are present in the mastoid apex. Posteriorly, the cells almost reach the occipito-mastoid suture. The largest cells are the most anteriorly located. In terms of disposition and size, pneumatization is very similar in the right and left temporal bones. The disposition of the

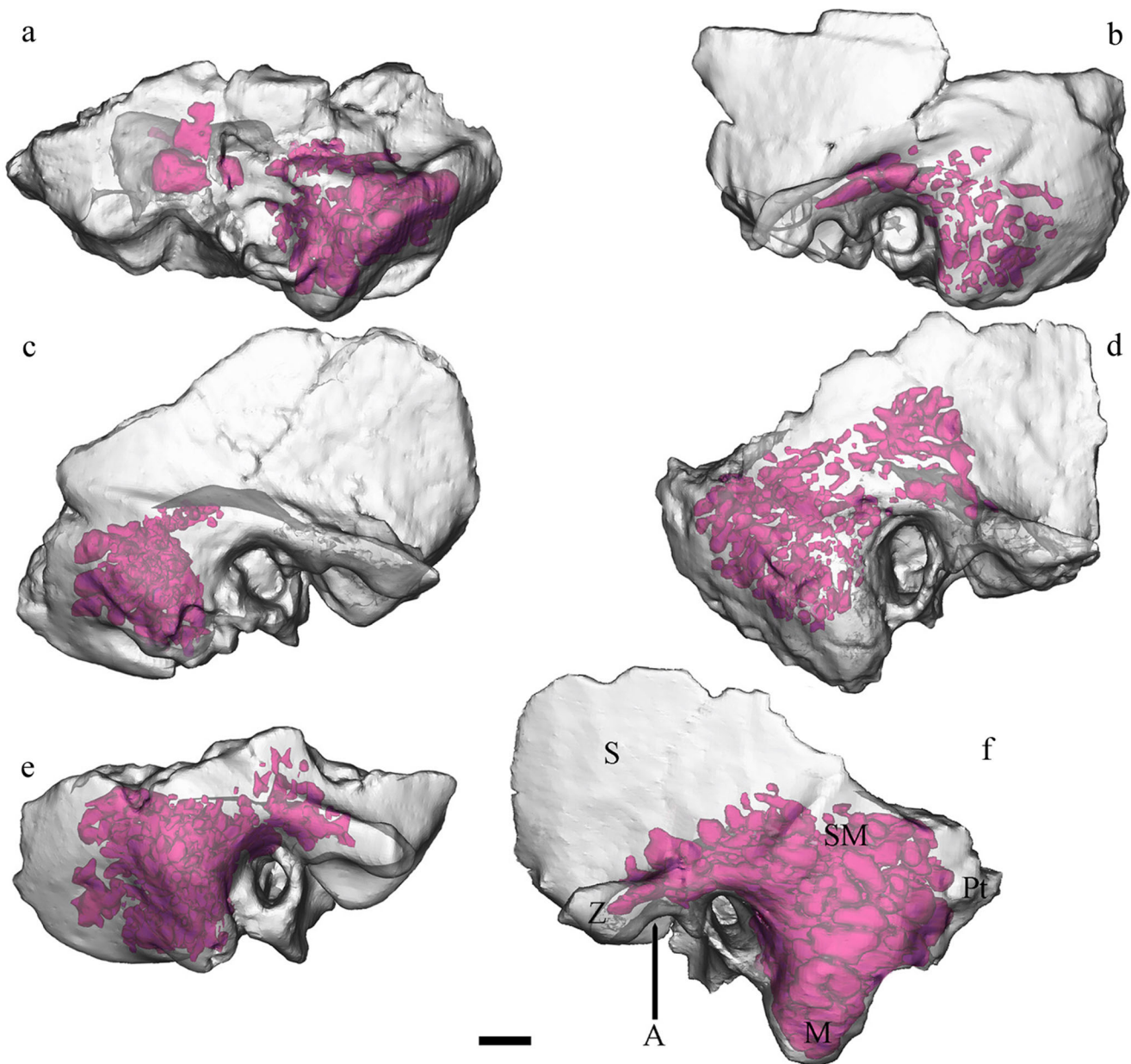


Fig. 2 Lateral views of the 3D reconstructions of the temporal bone and pneumatization: KNM-ER 1805 (a, left temporal bone), KNM-ER 1813 (b, left temporal bone), KNM-ER 3733 (c, right temporal bone), KNM-ER 3883 (d, right temporal bone), KNM-WT 15000 (e, right temporal bone) and *Homo sapiens* (f, Afalou 2, left temporal bone). The temporal bones are shown in grey; pneumatization is visible by transparency and is shown in a darker colour. Scale bar = 1 cm. The areas coded in Table 1 are labelled on the *Homo sapiens* temporal bone: Z (zygomatic process), A (articular tubercle), S (squamous temporal), SM (squamomastoid area), M (mastoid apex), Pt (posterior temporal); the petrosal and the petrosal apex are not visible under this orientation / *Vues latérales des reconstructions 3D de l'os temporal et de sa pneumatisation* : KNM-ER 1805 (a, temporal gauche), KNM-ER 1813 (b, temporal gauche), KNM-ER 3733 (c, temporal droit), KNM-ER 3883 (d, temporal droit), KNM-WT 15000 (e, temporal droit) et *Homo sapiens* (f, Afalou 2, temporal gauche). Les os temporaux sont représentés en gris, la pneumatisation est visible par transparence et représentée en couleur plus foncée. Echelle = 1 cm. Les zones codées dans le tableau 1 sont illustrées sur l'os temporal d'Homme moderne : Z (processus zygomatic), A (tubercule articulaire), S (écaille temporelle), SM (zone squamomastoïde), M (apex mastoïdien), Pt (partie postérieure du temporal) ; l'os pétreux et son apex ne sont pas visibles selon cette orientation.

pneumatic cells in OH 5 (Fig. 1e) is very similar to that observed in KNM-WT 17000. The only difference is that pneumatization has spread slightly more vertically above the EAM in OH 5. SK 48 is heavily mineralized, filled with sediment and partially crushed. Pneumatic cells were observed in the mastoid area and above the EAM. In TM 1517, the pneumatized area is not very well preserved; moreover, some sediment and diagenetic modifications have affected the preservation of the original internal structure of the bone. Pneumatic cells are present above the mandibular fossa but do not extend into the upper part of the squamous temporal or anteriorly to this area. They are clearly present in the posterior and medial parts of the temporal.

In KNM-ER 1805 (Fig. 2a), many relatively small pneumatic cells are present in the petromastoid area. The most anterior cells are large and located in the inferior extension of the temporal squama, just above the mandibular fossa. These are also the topmost cells, extending vertically into the middle of the temporal squama. Medially, pneumatization reaches the apex of the petrosal. Inferiorly, pneumatic cells are present in the mastoid process and one cell has spread into the upper part of the juxtamastoid eminence. The cells in the area posterior to the parietal notch are large, and the above-mentioned cell is also thick. The anterior extension of pneumatization in KNM-ER 1813 (Fig. 2b) corresponds to a large cell located at the medial extension of the zygomatic process, just above the lateral part of the mandibular fossa. Some cells are present in the lowest part of the temporal squama, in the area surrounding the EAM. Superiorly, pneumatization does not extend far above the supramastoid crest and there is no evidence of propagation into the temporal squama. Many cells are present in the mastoid area, extending inferiorly into its apex and into the upper part of the juxtamastoid eminence. The cells do not extend posteriorly towards the petromastoid area.

In KNM-ER 3733 (Fig. 2c), pneumatization is restricted to the petromastoid area. There is no evidence of cell propagation in front of the posterior wall of the EAM and above the level of the supramastoid crest. The petrous apex seems to be pneumatized, as is the mastoid apex. Significant pneumatization of the petromastoid area is also apparent in KNM-ER 3883 (Fig. 2d), and has also spread into the postero-medial extension of the zygomatic process, as well as into the temporal squama in the entire area above the EAM, reaching the endocranial extension of the parieto-temporal suture. There is no evidence of pneumatization of the other areas of the temporal squama. KNM-WT 15000 (Fig. 2e) is significantly pneumatized in the petromastoid area. Anteriorly, pneumatic cells have spread as far as the roof of the articular tubercle. Superiorly, they have reached the middle of the temporal squama, just in front of the EAM. Inferiorly, pneumatic cells are present in the mastoid apex

and in the summit of the juxtamastoid eminence. Others are also present just behind the mastoid relief. Further development of pneumatization would have been expected if this immature individual had reached adulthood. In KNM-ER 3733 and 3883 and KNM-WT 15000, limited but apparent left-right variation in pneumatization can be observed.

Summary and conclusions

Any summary of current knowledge on the characteristics of temporal bone pneumatization in hominids will inevitably be incomplete because of the relatively low intra- and interspecies variation documented to date in fossil hominins. Additional work is needed to understand how pneumatization varies and to further explore the possible phylogenetic implications. However, our description of the temporal bone pneumatization pattern in some key specimens from Africa already allows a more detailed description of the variation and evolution of this feature among hominins (Table 1). We had previously reported [24-26] that some variation exists among Asian *Homo erectus* as pneumatization is very developed in the Zhoukoudian specimens, although this is not the case with the Ngandong and Sambungmacan fossils. Moreover, although temporal bone pneumatization shows some individual variability, a similar pattern of distribution was found in all adult Neandertal individuals from Krapina and Western Europe, in which pneumatization is mainly restricted to most parts of the petromastoid areas. Finally, temporal bone pneumatization varies greatly in modern humans. It is generally limited to the mastoid, perilabyrinthine and petrous regions, while propagation into the squamous temporal is rare and not extensive [12-23].

Contrary to previous suggestions [1-8], the specimens analysed here and attributed to *Australopithecus africanus* and *Paranthropus* do not display the ape-like pattern of pneumatization as found in African great apes (e.g., Fig. 1a and b). These exhibit extensive pneumatization, which invades the whole temporal bone. On the contrary, all the hominins studied here display less pneumatization of the temporal bone than great apes. More specifically, pneumatization in the specimens of *Australopithecus africanus* (N = 2) and *Paranthropus* (N = 4) never invades the entire temporal squama. We did not discern any clear variation in the pattern of pneumatization among the 4 specimens from the 3 different species of the genus *Paranthropus*. More generally, *Paranthropus* appears to be the only hominin with a partly pneumatized zygomatic process. When considering the anatomical peculiarities of the temporal bone, the distribution of pneumatization in *Paranthropus* seems to be unique when compared with *Australopithecus*, but also with other hominins. In this light, the much debated taxonomic attribution of KNM-ER 1805 [e.g., 3,29-30] deserves

some attention. This specimen is generally considered as an early *Homo*. Although analysis of its temporal bone pneumatization will not end this discussion, the pattern of distribution in this specimen (Fig. 2a) is more similar to what we observed in *Paranthropus* (very large cells in the temporal squama, which are located in a very anterior position, and large cells at the posterior extension of the temporo-nuchal crest on the temporal bone) than to early *Homo* and *Homo erectus s.l.* (this study; [24-26]). Moreover, pneumatization of the temporal bone of *Australopithecus sediba* [11], which is yet to be fully described, is not a *Homo*-like feature as at least the specimens attributed to *Australopithecus africanus* analysed here share this supposedly derived reduced pneumatization. Finally, in early *Homo* (KNM-ER 1813) and African *Homo erectus/Homo ergaster* (N = 3), pneumatization is well developed in the petromastoid area. Pneumatic cells may be present above the articular tubercle in the squamous temporal (Fig. 2a and d), but pneumatization has

not invaded the most anterior part of the squamous temporal. Similarly, we did not observe pneumatization in the anterior part of the articular tubercle or in the zygomatic and tympanic processes, the lower part of the juxtamastoid eminence or the area close to the occipito-mastoid suture. This pattern is comparable to what was previously observed in Asian *Homo erectus* and *Homo sapiens* (Table 1).

This preliminary study needs to be followed by others. CT and micro-CT data are a useful tool to identify anatomical features, as they reveal internal and hidden features. However, the resolution of the imaging dataset can be a limiting factor depending on the feature to be observed [31], and researchers should be cautious when they detail fine anatomical features with imaging datasets that have insufficient resolution. Further evaluations of variations in temporal bone pneumatization in African hominins and their value for taxonomic attribution are to be expected from analyses of the same specimens, using higher-resolution data and new

Table 1 Summary of the distribution of pneumatization in the different anatomical areas of the temporal bone in adult great apes and fossil hominins (see Fig. 2f for the location of the various areas) / *Résumé de la distribution de la pneumatization dans les différentes parties anatomiques de l'os temporal chez les grands singes adultes et les hominins fossiles (se reporter à la fig. 2f pour la localisation visuelle de ces différentes parties)..*

	Zygomatic process	Articular tubercle	Squamosal	Petrosal	Petrosal apex	Squamomastoid area	Mastoid apex	Posterior temporal
African great apes [9-10 and 27-28]	++	++	++	++	++	++	++	++
<i>Australopithecus africanus</i> (N=2)	x	+	+	++	?	++	++	+
<i>Paranthropus</i> (N=4)	+	++	+	++	+	++	++	++
early <i>Homo</i> (KNM-ER 1813)	x	+	x	++	?	++	++	x
<i>H. erectus/H. ergaster</i> Africa (N=3)	x	+	+	++	+	++	++	+
<i>H. erectus</i> Zhoukoudian (N=4) [25]	?	+	+	++	+	++	++	++
<i>H. erectus</i> Ngangong/Sambungmacan (N=5) [24]	x	x	x	+	-	++	-	x
modern humans [12-26]	-	-	-	++	+	++	++	-
Neandertals (N=25) [26]	x	x	x	++	-	++	-	x

Coding for the temporal bone pneumatization: x: absent, -: rare, +: frequent/moderate, ++: very developed. The localisation of the different areas of the temporal bone is illustrated on the Figure 2f / Codage x : absente, - : rare, +: fréquente/modérée, ++: très développée. Se reporter à la fig. 2f pour la localisation visuelle de ces différentes parties.

quantification methods [32] for species that are not yet documented for this feature (e.g., *Sahelanthropus* or *Ardipithecus ramidus* [33]) and for several additional specimens of the other species. These analyses will also contribute to the ongoing debate on the developmental and/or functional origin of pneumatization [34,35].

Acknowledgements This research was supported by the Paul Broca II project on “The evolution of cerebral asymmetry in *Homo sapiens*”, conducted under the 6th EU Framework Programme for Research and Development. We are grateful to José Braga, Emma Mbuja and Gerhard Weber for providing CT data. Thanks also to Dominique Grimaud-Hervé, Emmanuel Gilissen, Wim Wendelen, Walter Coudyzer and Patrick Semal for their various contributions to our research. The comments from two anonymous reviewers and an associate editor greatly improved this paper.

References

- Zonneveld F, Wind, J (1985) High-resolution CT of fossil hominid skulls: a new method and some results. *Hominid Revolution: Past, Present and Future*. Alan R Liss, pp 427-436
- Grine FE, Strait DS (1994) New hominid fossils from Member 1 “Hanging Remnant”, Swartkrans Formation, South Africa. *J Hum Evol* 26:57–75
- Kimbel WH, White TD, Johanson DC (1984) Cranial morphology of *Australopithecus afarensis*: a comparative study based on a composite reconstruction of the adult skull. *Am J Phys Anthropol* 64:337–88
- Kennedy GE (1991) On the autapomorphic traits of *Homo erectus*. *J Hum Evol* 20:375–412
- White TD, Suwa G, Asfaw B (1994) *Australopithecus ramidus*, a new species of early hominid from Aramis, Ethiopia. *Nature* 371:306–12
- Ward CV, Leakey M, Walker A (1999) The new hominid species *Australopithecus anamensis*. *Evol Anthropol* 7:197–205
- Sherwood RJ, Ward SC, Hill A (2002) The taxonomic status of the Chemeron temporal (KNM-BC 1). *J Hum Evol* 42:153–184
- Nevell L, Wood B (2008) Cranial base evolution within the hominin clade. *J Anat* 212:455–68
- Sherwood RJ (1995) The hominid temporal bone: ontogeny and phylogenetic implications. Ph.D. Dissertation, Kent State University, USA
- Sherwood RJ (1999) Pneumatic processes in the temporal bone of chimpanzee (*Pan troglodytes*) and gorilla (*Gorilla gorilla*). *J Morphol* 241:127–37
- Berger LR, de Ruiter DJ, Churchill SE et al (2012) *Australopithecus sediba*: a new species of *Homo*-like australopithecids from South Africa. *Science* 328:195–204
- Turner A, Porter WA (1922) The structural type of the mastoid process based upon the skiagraphic examination of 1000 crania of various races of mankind. *J Laryngol* 37:115–21
- Allam AF (1969) Pneumatization of the temporal bone. *Annl. Otol Rhinol Laryngol* 78:49–64
- Wolfowitz BL (1974) Pneumatization of the skull of the South African negro. Ph.D. Dissertation, University of the Witwatersrand, Johannesburg, South Africa
- Schulter FP (1976) A comparative study of the temporal bone in three populations of man. *Am J Phys Anthropol* 44:453–468
- Schulter-Ellis FP (1979) Population differences in cellularity of the mastoid process. *Acta Oto-laryngol* 87:461–5
- Virapongse C, Sarwar M, Bhimani S et al (1985) Computed tomography of temporal bone pneumatization: 1. Normal pattern and morphology. *Am J Roentgenol* 147:473–81
- Zonneveld F (1987) Computed Tomography of the temporal bone and orbit. Urban & Schwarzenberg, Munich
- Scheuer L, Black S (2000) Developmental juvenile osteology. Academic Press, San Diego
- Hill CA (2008) Evolutionary and developmental history of temporal bone pneumatization in hominids. Ph.D. Dissertation, Pennsylvania State University, USA
- Hill CA, Richtsmeier JT (2008) A quantitative method for the evaluation of three-dimensional structure of temporal bone pneumatization. *J Hum Evol* 55:682–90
- Hill CA (2011) Ontogenetic changes in temporal bone pneumatization in humans. *Anat rec* 7:1103–15
- Bronoosh P, Shakibafard A; Mokhtare MR, Munesi Rad T (2014) Temporal bone pneumatization: a computed tomography study of pneumatized articular tubercle. *Clinical radiology* 69:151–6
- Balzeau A, Grimaud-Hervé D (2006) Cranial base morphology and temporal bone pneumatization in Asian *Homo erectus*. *J Hum Evol* 51:350–359
- Balzeau A, Grimaud-Hervé D, Sémah F (2008) Characteristics and variation of the temporal bone pneumatization in Asian *Homo erectus*. In: Pautreau, J.P., Coupey, A.S, Zeitoun, V., Rambault, E., (Eds), *From Homo erectus to the living traditions*. Choice of papers from the 11th conference of the European Association of Southeast Asian Archaeologists. Eurasea, Chiang Mai, pp. 21-7
- Balzeau A, Radovčić J (2008) Variation and modalities of growth and development of the temporal bone pneumatization in Neandertals. *J Hum Evol* 54:546–67
- Balzeau A, Gilissen E, Wendelen W, Coudyzer W (2009) Internal cranial anatomy of the type specimen of *Pan paniscus* and available data for study. *J Hum Evol* 56:205–8
- Balzeau A, Gilissen E (2010) Endocranial shape asymmetries in *Pan paniscus*, *Pan troglodytes* and *Gorilla gorilla* assessed via skull based landmark analysis. *J Hum Evol* 59:54–69.
- Thompson JL (1993) The unusual cranial attributes of KNM-ER 1805 and their implication for studies of sexual dimorphism in *Homo habilis*. *Hum Evol* 8:255–63
- Prat S (2002) Anatomical study of the skull of the Kenyan specimen KNM-ER 1805: a reevaluation of its taxonomic allocation? *C R Palevol* 1:27–33
- Balzeau A, Crevcoeur I, Rougier H et al (2010) Applications of imaging methodologies to paleoanthropology: Beneficial results relating to the preservation, management and development of collections. *C R Palevol* 9:265–75
- Hill CA, Richtsmeier JT (2008) A quantitative method for the evaluation of three-dimensional bone pneumatization. *J Hum Evol* 55:682–90
- Suwa G, Asfaw B, Kono RT, et al (2009) The *Ardipithecus ramidus* skull and its implications for hominid origins. *Science* 326,68e1-e7
- Witmer LM (1997) The evolution of the antorbital cavity of archosaurs: a study in soft-tissue reconstruction in the fossil record with an analysis of the function of pneumaticity. *J Vert Paleontol* 17:1–74
- Zollikofer CPE, Weissmann JD (2008) A morphogenetic model of cranial pneumatization based on the invasive tissue hypothesis. *Anat rec* 11:1446–54